Medical Oncology (2025) 42:105
https://doi.org/10.1007/s12032-025-02653-0

ORIGINAL PAPER

# αKG-induced oxidative stress and mTOR inhibition as a therapeutic strategy for liver cancer

**Sung Kyung Choi[1] · Myoung Jun Kim[1] · Jueng Soo You[1,2]**

Received: 13 December 2024 / Accepted: 24 February 2025 / Published online: 13 March 2025
© The Author(s) 2025


## Abstract

Despite the availability of targeted therapies, liver cancer remains a severe health burden. The need for adjuvant therapy to improve treatment efficacy and prevent recurrence is emerging. Alpha-ketoglutarate (αKG) is an intermediate in the tricarboxylic acid cycle and a cofactor for various oxygenases. A critical role of this multifunctional metabolite has started to be revealed in physiological and pathological conditions. We found that αKG exerts various anti-tumor effects in liver cancer cells. Our kinetic transcriptome study suggested that increasing reactive oxygen species and inhibiting mTORC1 signaling underlies. Indeed, αKG treatment elevated oxidative stress and induced DNA damage, presumably caused by early downregulation of the antioxidant gene SLC7A11. Further, we validated impaired mTOR signaling and decreased cellular energy production. This unique mechanism underscores αKG's potential as a liver cancer therapy by harnessing oxidative stress and disrupting metabolic signaling. These findings could provide valuable insights into further exploration of αKG as a promising therapeutic agent in liver cancer.


**Keywords** Liver cancer · Alpha-Ketoglutarate · mTOR · Anti-tumor · ROS · ATP

**Abbreviations**

| | |
|---|---|
| αKG | Alpha-ketoglutarate |
| ROS | Reactive oxygen species |
| mTOR | Mechanistic target of rapamycin |
| JmjC | Jumonji C |
| DCFH-DA | 2′,7′-Dichlorofluorescein diacetate |
| $x\_c^-$ | Cystine/glutamate antiporter system |
| OXPHOS | Oxidative phosphorylation |
| ATP | Adenosine triphosphate |
| NAFLD | Non-alcoholic fatty liver disease |
| TCA | Tricarboxylic acid |

## Introduction

Liver cancer is a prevalent malignancy, and its incidence is closely linked to chronic infections with hepatitis viruses, as well as lifestyle factors such as alcohol consumption and metabolic disorders [1]. These etiological factors contribute to the genomic instability and molecular complexity observed in liver cancer, resulting in limited therapeutic success for advanced-stage patients [2, 3]. Multi-targeted kinase inhibitors, such as sorafenib and lenvatinib, provide benefits in liver cancer treatment but often come with significant side effects, underscoring the need for novel treatments [4, 5]. Therefore, research focused on discovering more effective treatments or adjuvant therapies is essential to improve treatment outcomes for patients with liver cancer.

Alpha-ketoglutarate (αKG), a critical intermediate in the tricarboxylic acid (TCA) cycle, plays an integral role in cellular metabolism [6]. As a substrate in the TCA cycle, αKG facilitates the generation of reducing equivalents, such as NADH and $FADH_2$, which drive oxidative phosphorylation and ATP production in the electron transport chain [7, 8]. This process is essential for maintaining cellular energy supply, particularly in metabolically active cells [8, 9]. Interestingly, αKG inhibits ATP synthase activity under energy stress or nutrient deprivation, thereby limiting ATP production [10]. αKG's balanced involvement in energy production underscores its significance. In this context, αKG modulates cellular metabolic flux by regulating the mechanistic target of rapamycin (mTOR) pathway, a key regulator of cell growth and metabolism [11].

✉ Jueng Soo You
jsyou@kku.ac.kr

1 Department of Biochemistry, School of Medicine, Konkuk University, Chungju-Si 27478, Chungcheongbuk-Do, Korea

2 Research Institute of Medical Science, KU Open Innovation Center, Chungju-Si 27478, Chungcheongbuk-Do, Korea

The effect of αKG on mTOR signaling is highly context-dependent. Under nutrient-rich conditions, αKG activates mTOR, enhancing protein synthesis and promoting cell proliferation [12, 13]. Conversely, under metabolic stress, αKG suppresses mTOR activity to conserve ATP and prioritize survival pathways [10, 14].

αKG exhibits a context-dependent regulation of reactive oxygen species (ROS) levels. In normal states, αKG enhances antioxidant defenses by scavenging ROS and promoting glutathione synthesis, thereby preventing oxidative damage [15]. However, in cancer cells, αKG selectively increases ROS levels, disrupting redox homeostasis and pushing ROS beyond tolerable thresholds, leading to cellular dysfunction, ferroptosis, and apoptosis [16, 17]. The pro-apoptotic effects of αKG are further attributed to ROS-mediated ER stress and JNK/caspase-9 activation, highlighting these pathways as key mechanisms underlying αKG-induced cell death in cancer [18, 19]. αKG also serves as a critical cofactor for epigenetic enzymes, including TET dioxygenases and Jumonji C (JmjC) domain-containing histone demethylases [20]. Given that these enzymes regulate gene expression by modifying DNA and histone demethylation, their effects are expected to be genome-wide [21, 22]. Despite these insights, the role of αKG in epigenetic regulation, specifically in liver cancer, remains poorly understood.

This study explored the molecular mechanisms underlying the anticancer effects of αKG in liver cancer cells. Through kinetic transcriptome analysis, we demonstrated that αKG treatment significantly increased intracellular ROS levels, which subsequently inhibited the mTOR pathway, depleted ATP, and ultimately induced apoptosis. Our findings suggest that αKG could be a promising therapeutic strategy targeting unique vulnerabilities in liver cancer.

## Materials and methods

### Cell lines and culture

The liver cancer cell lines HepG2 and Huh7 were used in this study. HepG2 cells, widely utilized as a model for hepatocellular carcinoma, have also been referred to as hepatoblastoma cells in some studies (PubMed: 233137, 6248960, and 19751877). Huh7, derived from a well-differentiated hepatocellular carcinoma, is commonly employed to study liver cancer pathology and therapeutic responses. Both cell lines were kindly provided by Professor Suk Woo Nam from the Catholic University. Cells were maintained in DMEM (WELGENE, Cat. No. LM001-05) supplemented with 10% fetal bovine serum (WELGENE, Cat. No. S001-07) and 1% penicillin–streptomycin (GenDEPOT, Cat. No. CA005-010), incubated at 37 °C in a 5% $CO_2$ atmosphere.

### αKG treatment

The αKG compound used was cell-permeable dimethyl-αKG (DM-αKG, Sigma-Aldrich, Cat. No. 349631-5G). The concentrations and treatment durations are detailed in the corresponding figure legends.

### Cell proliferation assay

Cells were seeded at a density of $5 \times 10^4$ cells/well in six-well plates. Daily cell counts were conducted using a Trypan Blue exclusion assay, where 10 µL of cell suspension was mixed with 10 µL of Trypan Blue (Thermo Fisher Scientific, Cat. No. 15250061), and viable cells were counted using a hemocytometer under a light microscope.

### RNA extraction and RT-qPCR

Total RNA was extracted using the easy-BLUE™ Total RNA Extraction Kit (iNtRON, #17061) following the manufacturer's protocol. Complementary DNA (cDNA) was synthesized from 1 µg of total RNA using the High Capacity cDNA Reverse Transcription Kit (Applied Biosystems, #4368813), according to the manufacturer's instructions. Real-time quantitative PCR (RT-qPCR) was performed using the CFX Connect™ Real-Time PCR Detection System (BIO-RAD, Hercules, CA, USA) with iQ™ SYBR® Green Supermix (BIO-RAD, #170-8882AP). The following primers were used for SLC7A11: Forward 5′-CTG AGC GGC TAC TGG GAA AT-3′, Reverse 5′-TGG TAG AGG AGT GTG CTT GC-3′.

### Western blot analysis

Cells were lysed in RIPA buffer (CELLNEST, Cat. No. CNR001-0100) supplemented with protease inhibitors (Abbkine, Cat. No. BMP1001) and sonicated briefly to ensure complete lysis. Protein concentrations were measured with the Bradford assay (Bio-Rad, Cat. No. 5000006). Equal protein amounts (30 µg) were loaded onto 8–15% SDS-PAGE gels and electrophoresed. After transfer to nitrocellulose membranes (Bio-Rad, Cat. No. 1620115), membranes were blocked with 10% skim milk (Difco, Cat. No. 232100) in TBS-T for 1 h, then probed overnight at 4 °C with primary antibodies (Supplementary Table 1). Membranes were incubated with HRP-conjugated secondary antibodies (1:10,000) at room temperature for 1 h. Blots were developed using ECL (Abfrontier, Cat. No. LF-QC0103), and band intensities were quantified using ImageJ software.

## Apoptosis

Apoptosis was measured using an Annexin V-FITC Apoptosis Detection Kit (BD Biosciences, Cat. No. 556547). Cells were washed in PBS, and then resuspended in 500 μL binding buffer. After adding 5 μL of Annexin V-FITC and 5 μL of PI, the samples were incubated in the dark for 15 min. Stained cells were analyzed using a BD Accuri C6 flow cytometer (BD Biosciences), and data were processed with FlowJo software.

## Wound healing assay

Cells were cultured to confluence in six-well plates and starved overnight in serum-free DMEM. A scratch was made with a sterile 200 μL pipette tip, and wells were rinsed with PBS to remove detached cells. Images were taken immediately (0 h) and at 24, 48, and 72 h using a light microscope (OLYMPUS IX71 Research Inverted Microscope), and gap widths were measured to assess migration.

## Microarray

Labeled cRNA was generated from 1–5 μg of total RNA using Agilent's Quick Amp Labeling Kit. After fragmentation, 1.65 μg of labeled cRNA was hybridized onto the Agilent expression microarray, following the manufacturer's protocol. The arrays were scanned using the Agilent Technologies G4900DA SG12494263 scanner. Data export, processing, and analysis were performed using Agilent Feature Extraction software (v11.0.1.1). The microarray data set was sourced from the NCBI Gene Expression Omnibus (GEO) database (accession no. GSE279001).

## ROS measurement

Cells were seeded into a 24-well plate and incubated for 24 h at 37 °C in a $CO_2$ incubator. After incubation, cells were washed with Hank's Balanced Salt Solution (HBSS, Sigma H6648) and treated with 20 μM carboxy-H2DCF-DA (Molecular Probes, #C-400) in HBSS, followed by incubation at 37 °C for 10 min. Excess carboxy-H2DCF-DA was removed by washing the cells with HBSS, and 1 mL of fresh HBSS was added. The cells were incubated for 120 min, then washed twice with cold HBSS, and lysed with 0.5% Triton X-100 (diluted in PBS) for 5 min. Fluorescence intensity was measured using a multi-well plate reader at an excitation wavelength of 485 nm and emission wavelength of 530 nm.

## Comet assay

DNA damage was assessed using the OxiSelect™ Comet Assay Kit (Cell Biolabs, Cat. No. STA-351) according to the manufacturer's protocol. Cells were embedded in low-melting-point agarose on comet slides and electrophoresed. DNA was stained with Vista Green DNA Dye (Cell Biolabs), and comet tail lengths were quantified using a fluorescence microscope (OLYMPUS IX71 Research Inverted Microscope).

## ATP level measurement

Intracellular ATP levels were quantified using the ATeam1.03-nD/nA/pcDNA3 plasmid (Addgene, Cat. No. 51958) transfected into cells. Fluorescence was measured using a microplate reader, and data were analyzed with ImageJ.

## Statistical analysis

Data are presented as mean ± SEM. Statistical significance was determined using a one-way ANOVA followed by Tukey's post hoc test for multiple comparisons, with significance levels set at $*P < 0.05$, $**P < 0.01$, and $***P < 0.001$. All experiments were performed in triplicate ($n = 3$) to ensure reproducibility. Statistical analyses were conducted using Prism.

# Result

## αKG reduces liver cancer cell viability by inhibiting growth and migration

To investigate the potential anti-tumor effects of αKG on liver cancer cells, we treated HepG2 and Huh7 cells with cell-permeable αKG (Dimethyl 2-oxoglutarate, DM-αKG) at varying concentrations and time points. Our results demonstrated a dose- and time-dependent decrease in cell viability in both cell lines, confirmed by significant inhibition of cell proliferation (Fig. 1A, B). This reduction in proliferation coincided with the activation of apoptotic pathways, as indicated by cleaved caspase-3 and confirmed by annexin V-FITC and propidium iodide co-staining, markers of early apoptosis (Fig. 1C, D). These findings suggest that αKG not only reduces proliferation but actively promotes programmed cell death. Furthermore, αKG impaired liver cancer cell migration, as demonstrated by wound healing assays, indicating an additional effect on tumor progression (Fig. 1E). Together, these results provide initial evidence that αKG exerts anti-tumor effects by inhibiting cell proliferation, inducing apoptosis, and reducing cell migration.

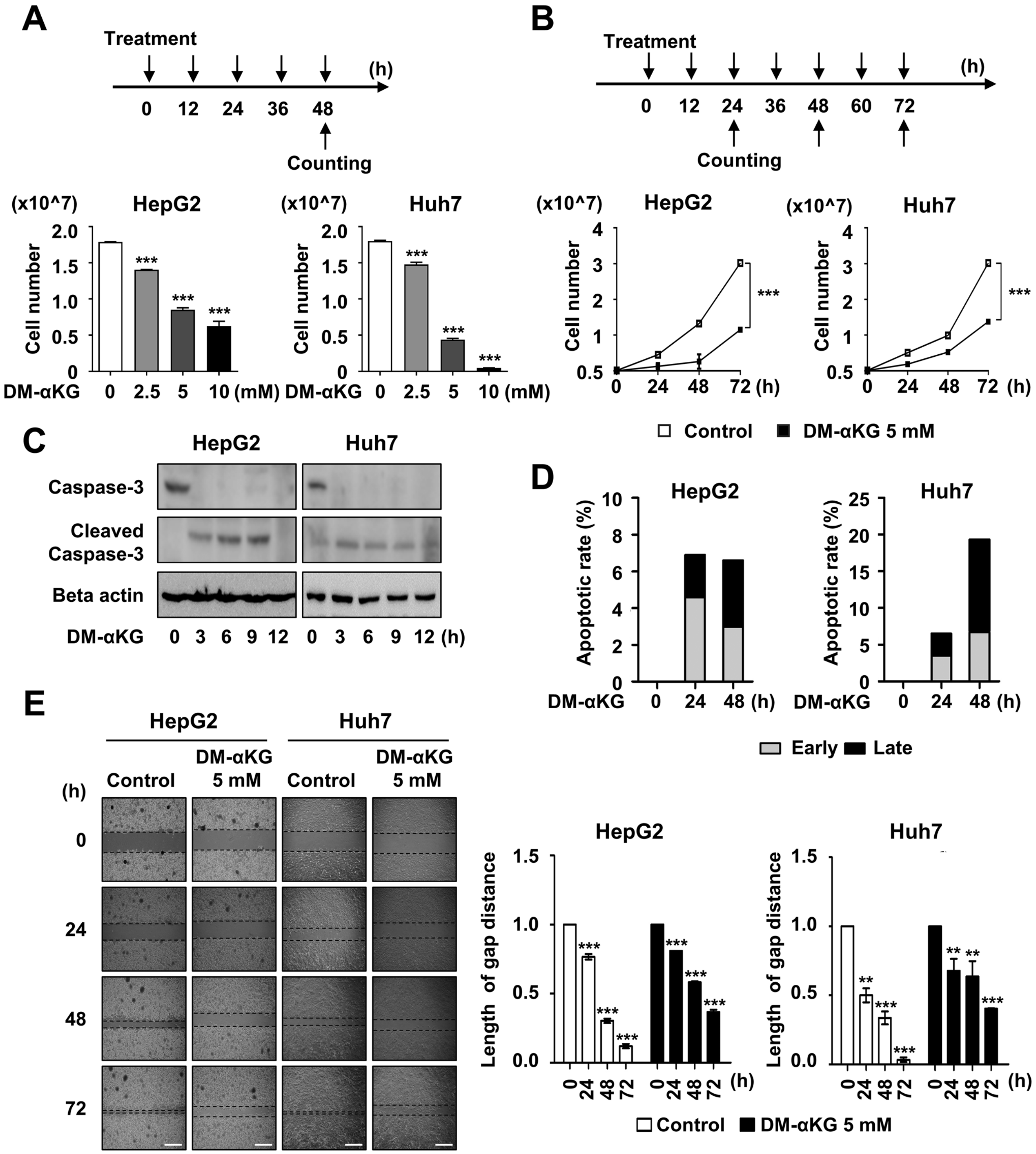


**Fig. 1** αKG exhibits anti-tumor effects. **A** Dose-dependent effect of DM-αKG on the proliferation of HepG2 and Huh7 cells (mean ± SEM, $^{***}p < 0.001$, $n = 3$). **B** Time-dependent effect of DM-αKG on the proliferation of HepG2 and Huh7 cells (mean ± SEM, $^{***}p < 0.001$, $n = 3$). **C** Protein levels of Caspase-3, Cleaved Caspase-3, and Beta actin in HepG2 and Huh7 cells following DM-αKG treatment. **D** Time-dependent induction of apoptosis in HepG2 and Huh7 cells treated with DM-αKG. **E** Time-dependent effect of DM-αKG on wound healing in HepG2 and Huh7 cells (mean ± SEM, $^{**}p < 0.01$, $^{***}p < 0.001$, $n = 3$) (Scale bar = 500 µm)

### Kinetic transcriptome analysis reveals early αKG-induced changes in ROS and mTORC1 signaling pathways in liver cancer

Previous studies have shown that αKG exerts anticancer effects by promoting prolyl hydroxylase (PHD) activity, destabilizing HIF-1α, and impairing hypoxic adaptation in certain cancer types, including breast, colon, and melanoma cancers and glioblastoma [23–25]. To determine whether this mechanism is operative in liver cancer, we investigated the cell type-specific effects of αKG on HIF-1α expression in liver cancer cells. Interestingly, αKG increased HIF-1α expression in HepG2 cells, which exhibit inherently low basal levels of HIF-1α, while it decreased HIF-1α expression in Huh7 cells, which have relatively high basal levels. These findings suggest that PHD-HIF-1α modulation may not be the primary pathway in liver cancer. Another established anti-tumor mechanism of αKG involves p53-mediated tumor suppression in pancreatic ductal adenocarcinoma [26]. However, we observed similar anti-tumor effects in both p53-wild-type and p53-deficient liver cancer cells, suggesting a p53-independent mechanism (Fig. 2A). Additionally, we did not observe autophagy inhibition, another known anticancer mechanism of αKG [27], indicating that autophagy is not a key pathway in liver cancer (Fig. 2A). To elucidate the underlying mechanism of the αKG anti-tumorigenic effect, we performed kinetic transcriptome analysis with control samples (0 h) in duplicate ($n = 2$), and all other time points (3, 6, 9, 12, 24, and 48 h) as single replicates ($n = 1$). We categorized the time points into four groups based on the duration of DM-αKG treatment and their distinct gene expression patterns: control (0 h), early (3 and 6 h), intermediate (9 and 12 h), and late (24 and 48 h) time points (Fig. 2B). Multidimensional scaling (MDS) plot showed the most distinct gene expression changes at early time points compared to control, while intermediate and late samples gradually converged toward the control, indicating a rapid but transient transcriptional response to DM-αKG (Fig. 2C). We also analyzed ferroptosis, another reported anticancer mechanism of αKG, and observed a significant reduction in SLC7A11 expression. However, the concomitant decrease in CHAC1 expression contradicted the expected ferroptosis-associated gene expression pattern (Fig. 2D). Gene set enrichment analysis (GSEA) further confirmed the absence of ferroptosis activation, as ferroptosis-related gene sets showed no significant enrichment (Fig. 2E). These findings suggest that ferroptosis is not the primary mechanism underlying αKG's anti-tumor effects in liver cancer cells. Based on expression profiles, we divided the genes into eight groups (Fig. 2F). The two majority groups showed early change and lasted: UUU (group 1) and DDD (group 8). The REACTIVE_OXYGEN_SPECIES pathway and MTORC1_SIGNALING pathway were the hallmark pathways of group 1 and group 8, respectively, in response to αKG treatment. Kinetic transcriptome analysis reveals upregulation of the REACTIVE_OXYGEN_SPECIES pathway, indicating increased oxidative stress within cells. Concurrently, consistent downregulation of the MTORC1_SIGNALING pathway suggests impaired cell growth and survival (Fig. 2G, H). These findings collectively propose that ROS-induced oxidative stress and mTORC1 signaling dysregulation are key mechanisms underlying the αKG-mediated anti-tumor response in liver cancer.

### αKG elevates ROS levels and induces DNA damage in liver cancer cells

To investigate the mechanism underlying αKG-induced cell death, we assessed ROS levels and DNA damage in liver cancer cells. αKG significantly increased ROS levels in both HepG2 and Huh7 cells, as measured by dichlorofluorescein diacetate (DCFH-DA) staining (Fig. 3A). Furthermore, a comet assay demonstrated increased DNA damage in αKG-treated cells compared to controls (Fig. 3B), suggesting that ROS-induced DNA damage may contribute to αKG-mediated apoptosis (Fig. 1C, D). Notably, we observed a significant downregulation of SLC7A11, a critical component of the cystine/glutamate antiporter system ($x\_c^-$) [28], upon αKG treatment (Fig. 3C), which was further confirmed by RT-qPCR, showing a significant, time-dependent reduction in SLC7A11 mRNA levels in both HepG2 and Huh7 cells (Fig. 3D).While global histone modifications, such as H3K4me3 and H3K9me3, remained relatively unchanged (Fig. 3E). Since the $x\_c^-$ system is essential for maintaining cellular redox balance, the selective repression of SLC7A11 by αKG likely enhances ROS production and oxidative stress.

### αKG suppresses mTOR signaling and reduces cellular ATP production

To validate the findings from our kinetic transcriptome analysis, we aimed to determine whether αKG directly regulates the mTOR pathway in liver cancer cells. GSEA revealed a significant downregulation of the HALLMARK_MTORC1_SIGNALING and PI3K_AKT_MTOR_SIGNALING pathways in response to αKG treatment (Fig. 4A). We observed a marked reduction in the phosphorylation levels of S6 (p-S6) and 4EBP1 (p-4EBP1) during the early phases (Fig. 4B), indicatkclaing early suppression of mTOR signaling by αKG. This mTOR inhibition correlated with the downregulation of gene sets involved in oxidative phosphorylation (OXPHOS), glycolysis, and ATP synthesis (Fig. 4C). αKG treatment caused a significant reduction in cellular ATP levels, similar to the effect of nutrient deprivation, indicating impaired energy metabolism (Fig. 4D). These findings

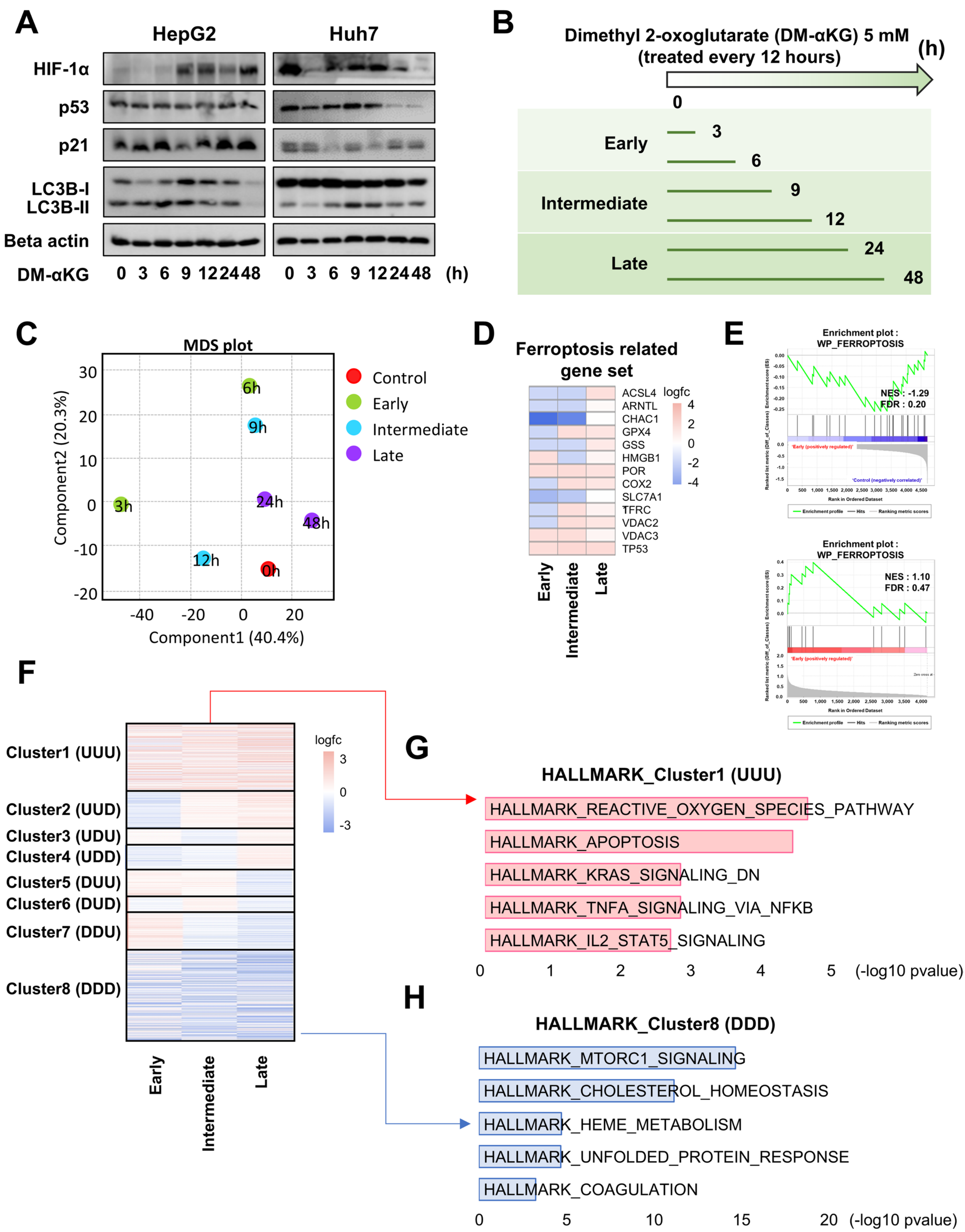
A
HepG2
Huh7
HIF-1α
p53
p21
LC3B-I
LC3B-II
Beta actin
DM-αKG
0 3 6 9 12 24 48
0 3 6 9 12 24 48 (h)
B
Dimethyl 2-oxoglutarate (DM-αKG) 5 mM
(treated every 12 hours)
(h)
0
Early
3
6
Intermediate
9
12
Late
24
48
C
MDS plot
Control
Early
Intermediate
Late
Component2 (20.3%)
Component1 (40.4%)
3h
6h
9h
12h
24h
48h
0h
D
Ferroptosis related gene set
logfc
ACSL4
ARNTL
CHAC1
GPX4
GSS
HMGB1
POR
COX2
SLC7A1
TFRC
VDAC2
VDAC3
TP53
Early
Intermediate
Late
E
Enrichment plot : WP_FERROPTOSIS
NES : -1.29
FDR : 0.20
Enrichment plot : WP_FERROPTOSIS
NES : 1.10
FDR : 0.47
F
Cluster1 (UUU)
Cluster2 (UUD)
Cluster3 (UDU)
Cluster4 (UDD)
Cluster5 (DUU)
Cluster6 (DUD)
Cluster7 (DDU)
Cluster8 (DDD)
logfc
Early
Intermediate
Late
G
HALLMARK_Cluster1 (UUU)
HALLMARK_REACTIVE_OXYGEN_SPECIES_PATHWAY
HALLMARK_APOPTOSIS
HALLMARK_KRAS_SIGNALING_DN
HALLMARK_TNFA_SIGNALING_VIA_NFKB
HALLMARK_IL2_STAT5_SIGNALING
(-log10 pvalue)
H
HALLMARK_Cluster8 (DDD)
HALLMARK_MTORC1_SIGNALING
HALLMARK_CHOLESTEROL_HOMEOSTASIS
HALLMARK_HEME_METABOLISM
HALLMARK_UNFOLDED_PROTEIN_RESPONSE
HALLMARK_COAGULATION
(-log10 pvalue)

◂**Fig. 2** DM-αKG alters transcriptome patterns in liver cancer cells. **A** Protein levels of HIF-1α, p53, p21, LC3B-I, LC3B-II, and Beta actin in HepG2 and Huh7 cells following DM-αKG treatment. **B** Schematic representation of the experimental design for DM-αKG treatment in liver cancer cells. **C** MDS plot showing transcriptome clustering of Control and DM-αKG-treated samples at different time points (3, 6, 9, 12, 24, and 48 h). **D** Expression changes in the ferroptosis-related gene set at early, intermediate, and late time points following DM-αKG treatment. Fold changes were calculated by normalizing each time point to the control condition. **E** GSEA analysis following DM-αKG treatment. **F** Gene expression changes in HepG2 cells after DM-αKG treatment. Time points (early, intermediate, and late) are categorized into upregulated and downregulated genes relative to the control (0 h), represented by eight groups. Fold changes were calculated by normalizing each time point to the control condition. U indicates upregulation, while D indicates downregulation. **G** Hallmark pathway analysis of genes consistently upregulated (UUU) across early, intermediate, and late time points following DM-αKG treatment in HepG2 cells. **H** Hallmark pathway analysis of genes consistently downregulated (DDD) across early, intermediate, and late time points following DM-αKG treatment in HepG2 cells

support a model where αKG inhibits mTOR signaling, leading to reduced ATP production likely via ROS-mediated mechanisms.

## Discussion

In this study, we explored the anticancer potential of αKG in liver cancer cells, focusing on early gene expression changes identified through kinetic transcriptome analysis. αKG treatment increased ROS levels, resulting in mTORC1 suppression, elevated oxidative stress, DNA damage, and reduced ATP production (Fig. 4E). These effects were validated through direct measurements of ROS, DNA damage, and ATP levels. Given the role of ROS as upstream regulators of mTOR signaling, downregulation of SLC7A11 might be the very upstream of effects. This study provides the first evidence of αKG's impact on liver cancer through this

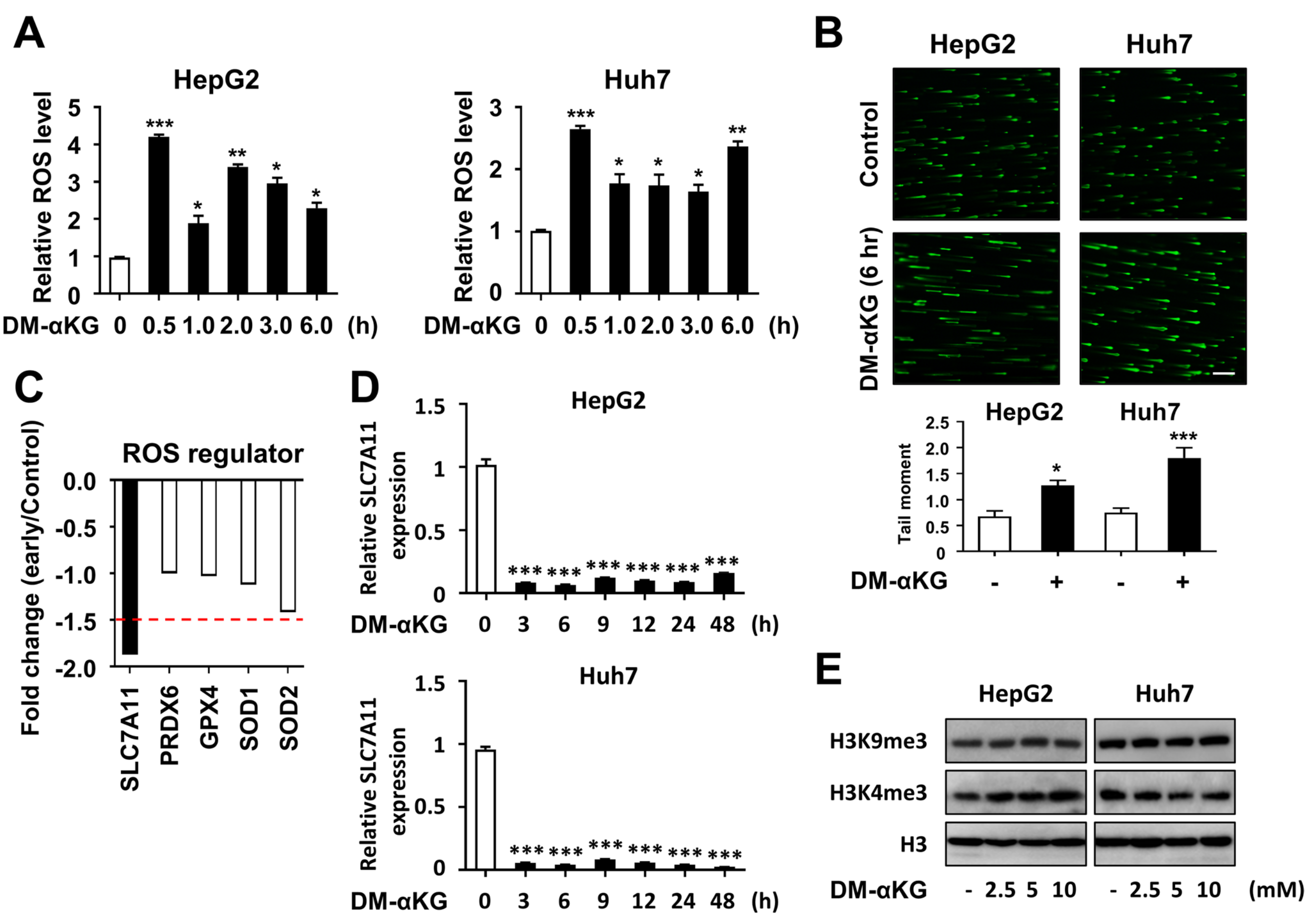


**Fig. 3** αKG treatment increases ROS levels. **A** ROS levels measured by DCF fluorescence intensity in HepG2 and Huh7 cells following DM-αKG treatment (mean ± SEM, $*p<0.05$, $**p<0.01$, $***p<0.001$, $n=3$). **B** Representative images of comet assay illustrating the degree of DNA damage and quantification of comet tail moments in HepG2 and Huh7 cells after DM-αKG treatment (mean ± SEM, $*p<0.05$, $***p<0.001$, $n=3$) (Scale bar = 200 μm). **C** Fold changes in ROS regulator expression based on microarray analysis following DM-αKG treatment. **D** Relative SLC7A11 expression in HepG2 and Huh7 cells following DM-αKG treatment (mean ± SEM, $***p<0.001$, $n=3$). **E** Protein levels of H3K4me3, H3K9me3, and H3 in HepG2 and Huh7 cells after DM-αKG treatment

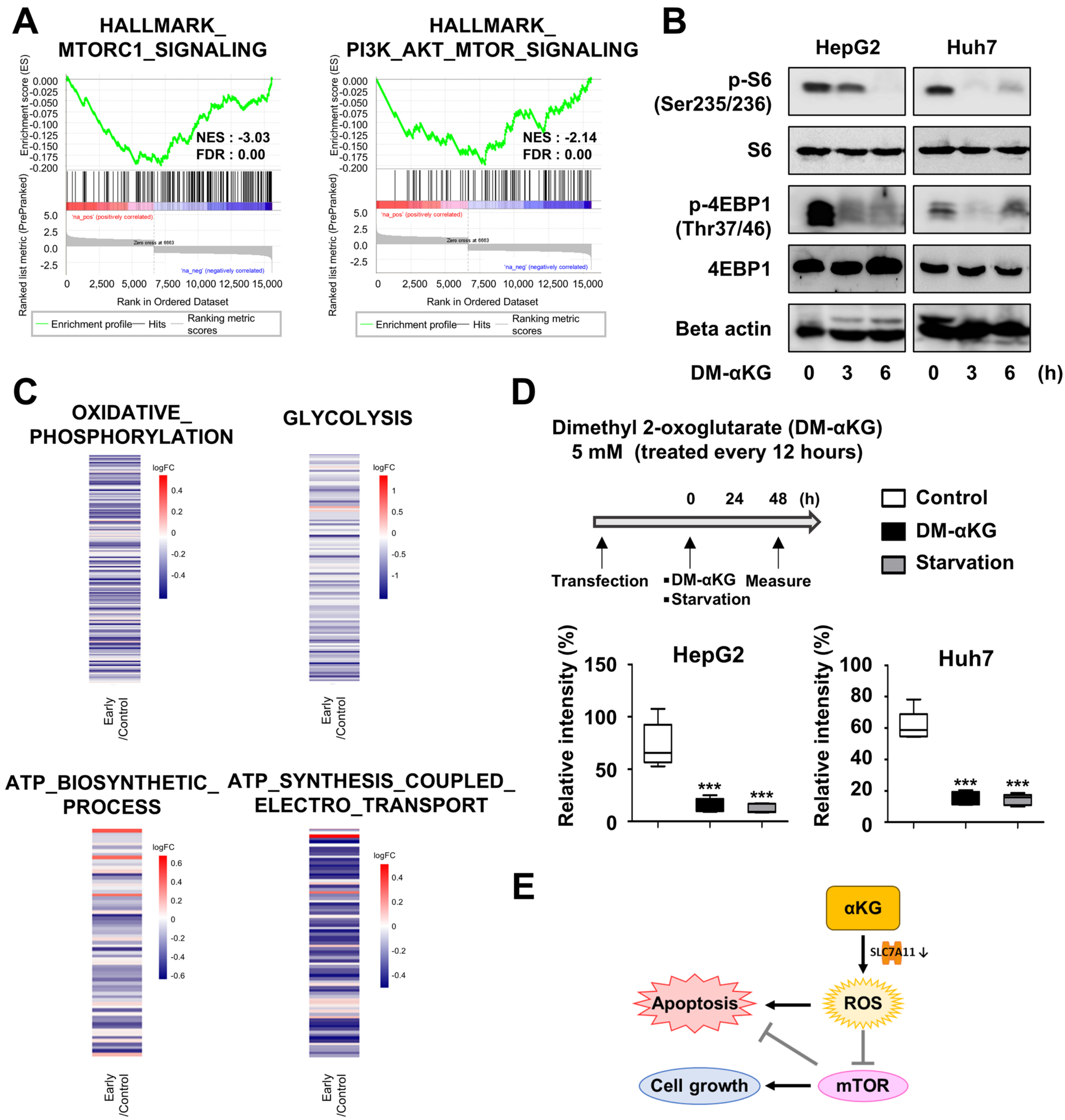


**Fig. 4** αKG suppresses mTOR signaling in liver cancer cells. **A** GSEA analysis following DM-αKG treatment. **B** Protein levels of p-S6, S6, p-4EBP1, 4EBP1, and Beta actin in HepG2 and Huh7 cells following DM-αKG treatment. **C** Gene expression changes observed at early time points post-DM-αKG treatment. The corresponding gene list is provided in the supplementary Table 2–5. **D** Schematic representation of the experimental design and ATP levels in HepG2 and Huh7 cells following DM-αKG treatment and under starvation conditions. **E** Summary diagram illustrating the overall effects of αKG treatment in liver cancer cells

mechanism, highlighting its therapeutic potential to disrupt key processes vital for tumor progression.

The therapeutic potential of αKG in non-alcoholic fatty liver disease (NAFLD) has been attributed to its beneficial effects on lipid metabolism and liver function [11, 29]. Preclinical studies have shown that cell-permeable αKG formulations can inhibit tumor growth in several cancer types [11, 30]. However, the anti-tumor potential of αKG in liver cancer has not been previously explored. This study is the first to demonstrate that αKG inhibits tumor growth in liver cancer cells, providing a novel and promising therapeutic strategy. The ROS-mediated inhibition of mTOR observed in liver cancer may offer valuable insights into new therapeutic approaches. Nevertheless, further research is needed to determine whether this ROS-mTOR pathway is specific to liver cancer or applicable to a broader range of tumor types. Although αKG may act as an epigenetic cofactor for the SLC7A11 gene, reducing its expression, other ROS-generating mechanisms should not be overlooked. To fully harness the therapeutic potential of αKG, a deeper understanding of the interplay between cellular redox balance and gene regulation is crucial.

Previous research has highlighted the use of mTOR inhibitors in liver cancer treatment. Traditional inhibitors, such as rapamycin and its analogs (rapalogs), target mTORC1 and have demonstrated efficacy in early-stage liver cancer [31]. However, their therapeutic efficacy in advanced liver cancer is limited by drug resistance, incomplete mTORC1 inhibition, and compensatory mTORC2 activation. Moreover, rapalogs are linked to adverse effects, such as immunosuppression and toxicity, which restrict their long-term use [32, 33]. Our study suggests that αKG may offer an alternative route to inhibit mTOR activity through a ROS-driven mechanism. However, the clinical potential of αKG as a substitute for rapalogs remains uncertain, and its efficacy in combination with other anticancer therapies needs further investigation. Additionally, our study was conducted in vitro, limiting the direct applicability of these results to in vivo settings. Further studies are needed to validate these findings in animal models and to evaluate potential off-target effects or toxicity.

## Conclusion

Our findings represent the first evidence that αKG can exert anti-tumor effects in liver cancer. Elevated ROS caused by presumable downregulation of SLC7A11 by αKG inhibits mTOR signaling. This disrupts cellular energy homeostasis, induces oxidative stress, and triggers DNA damage. Therefore, αKG offers a new therapeutic approach that could enhance the efficacy of current treatment strategies. Further exploration of the context-specific action mechanisms of αKG will improve its potential clinical applications for various diseases, including cancer.

**Supplementary Information** The online version contains supplementary material available at https://doi.org/10.1007/s12032-025-02653-0.

**Acknowledgements** Not applicable.

**Author contributions** S.K.C. (Sung Kyung Choi) contributed to the conceptualization, data curation, formal analysis, validation, writing, and editing of the manuscript. M.J.K. (Myoung Jun Kim) was responsible for data curation and formal analysis. J.S.Y. (Jueng Soo You) contributed to the conceptualization, data curation, formal analysis, supervision, funding acquisition, and writing and editing of the manuscript. All authors reviewed and approved the final manuscript.

**Funding** This research was supported by the Basic Science Research Program through the National Research Foundation of Korea (NRF), funded by the Ministry of Science, ICT & Future Planning (2021R1A2C4001833). This paper was written as part of Konkuk University's research support program for its faculty on sabbatical leave in 2024.

**Data availability** The accession number for gene expression data reported in this study is NCBI GEO: GSE279001.

## Declarations

**Conflict of interest** The authors declare no competing interests.

**Ethical approval** Not applicable.

**Consent to participate** Not applicable.

**Informed consent** All participants provided written informed consent before participation in the study.

**Open Access** This article is licensed under a Creative Commons Attribution-NonCommercial-NoDerivatives 4.0 International License, which permits any non-commercial use, sharing, distribution and reproduction in any medium or format, as long as you give appropriate credit to the original author(s) and the source, provide a link to the Creative Commons licence, and indicate if you modified the licensed material. You do not have permission under this licence to share adapted material derived from this article or parts of it. The images or other third party material in this article are included in the article's Creative Commons licence, unless indicated otherwise in a credit line to the material. If material is not included in the article's Creative Commons licence and your intended use is not permitted by statutory regulation or exceeds the permitted use, you will need to obtain permission directly from the copyright holder. To view a copy of this licence, visit http://creativecommons.org/licenses/by-nc-nd/4.0/.

## References

1. Llovet JM, et al. *Hepatocellular carcinoma*. Nat Rev Dis Primers. 2016;2:16018.
2. Shibata T. Genomic landscape of hepatocarcinogenesis. J Hum Genet. 2021;66(9):845–51.
3. Suresh D, et al. Therapeutic options in hepatocellular carcinoma: a comprehensive review. Clin Exp Med. 2023;23(6):1901–16.
4. Palmer DH. Sorafenib in advanced hepatocellular carcinoma. N Engl J Med. 2008;359(23):2498.
5. Kudo M, et al. Lenvatinib versus sorafenib in first-line treatment of patients with unresectable hepatocellular carcinoma: a randomised phase 3 non-inferiority trial. Lancet. 2018;391(10126):1163–73.
6. Legendre F, et al. Biochemical pathways to alpha-ketoglutarate, a multi-faceted metabolite. World J Microbiol Biotechnol. 2020;36(8):123.
7. He L, et al. The physiological basis and nutritional function of alpha-ketoglutarate. Curr Protein Pept Sci. 2015;16(7):576–81.
8. Martinez-Reyes I, Chandel NS. Mitochondrial TCA cycle metabolites control physiology and disease. Nat Commun. 2020;11(1):102.

9. Spinelli JB, Haigis MC. The multifaceted contributions of mitochondria to cellular metabolism. Nat Cell Biol. 2018;20(7):745–54.
10. Chin RM, et al. The metabolite alpha-ketoglutarate extends lifespan by inhibiting ATP synthase and TOR. Nature. 2014;510(7505):397–401.
11. Gyanwali B, et al. Alpha-Ketoglutarate dietary supplementation to improve health in humans. Trends Endocrinol Metab. 2022;33(2):136–46.
12. Duran RV, et al. Glutaminolysis activates Rag-mTORC1 signaling. Mol Cell. 2012;47(3):349–58.
13. Wang L, et al. Dietary supplementation with alpha-ketoglutarate activates mTOR signaling and enhances energy status in skeletal muscle of lipopolysaccharide-challenged piglets. J Nutr. 2016;146(8):1514–20.
14. Su Y, et al. Alpha-ketoglutarate extends Drosophila lifespan by inhibiting mTOR and activating AMPK. Aging (Albany NY). 2019;11(12):4183–97.
15. Bayliak MM, Lushchak VI. Pleiotropic effects of alpha-ketoglutarate as a potential anti-ageing agent. Ageing Res Rev. 2021;66:101237.
16. Cai Y, et al. alpha-KG inhibits tumor growth of diffuse large B-cell lymphoma by inducing ROS and TP53-mediated ferroptosis. Cell Death Discov. 2023;9(1):182.
17. Zou Z, et al. Induction of reactive oxygen species: an emerging approach for cancer therapy. Apoptosis. 2017;22(11):1321–35.
18. Wu F, et al. AKG induces cell apoptosis by inducing reactive oxygen species-mediated endoplasmic reticulum stress and by suppressing PI3K/AKT/mTOR-mediated autophagy in renal cell carcinoma. Environ Toxicol. 2023;38(1):17–27.
19. Kalawaj K, et al. Alpha ketoglutarate exerts in vitro anti-osteosarcoma effects through inhibition of cell proliferation, induction of apoptosis via the JNK and caspase 9-dependent mechanism, and suppression of TGF-beta and VEGF production and metastatic potential of cells. Int J Mol Sci. 2020;21(24):9406.
20. Xu W, et al. Oncometabolite 2-hydroxyglutarate is a competitive inhibitor of alpha-ketoglutarate-dependent dioxygenases. Cancer Cell. 2011;19(1):17–30.
21. Tran TQ, et al. alpha-Ketoglutarate attenuates Wnt signaling and drives differentiation in colorectal cancer. Nat Cancer. 2020;1(3):345–58.
22. Liu N, et al. Supplementation with alpha-ketoglutarate improved the efficacy of anti-PD1 melanoma treatment through epigenetic modulation of PD-L1. Cell Death Dis. 2023;14(2):170.
23. Hou P, et al. Intermediary metabolite precursor dimethyl-2-ketoglutarate stabilizes hypoxia-inducible factor-1alpha by inhibiting prolyl-4-hydroxylase PHD2. PLoS ONE. 2014;9(11):e113865.
24. Tennant DA, Gottlieb E. HIF prolyl hydroxylase-3 mediates alpha-ketoglutarate-induced apoptosis and tumor suppression. J Mol Med (Berl). 2010;88(8):839–49.
25. Zhao S, et al. Glioma-derived mutations in IDH1 dominantly inhibit IDH1 catalytic activity and induce HIF-1alpha. Science. 2009;324(5924):261–5.
26. Morris JPT, et al. alpha-Ketoglutarate links p53 to cell fate during tumour suppression. Nature. 2019;573(7775):595–9.
27. Baracco EE, et al. alpha-Ketoglutarate inhibits autophagy. Aging (Albany NY). 2019;11(11):3418–31.
28. Yan Y, et al. SLC7A11 expression level dictates differential responses to oxidative stress in cancer cells. Nat Commun. 2023;14(1):3673.
29. Aragones G, et al. Increased circulating levels of alpha-ketoglutarate in morbidly obese women with non-alcoholic fatty liver disease. PLoS ONE. 2016;11(4):e0154601.
30. Madala HR, et al. Nitrogen trapping as a therapeutic strategy in tumors with mitochondrial dysfunction. Cancer Res. 2020;80(17):3492–506.
31. Lu X, et al. Role of the mammalian target of rapamycin pathway in liver cancer: from molecular genetics to targeted therapies. Hepatology. 2021;73(Suppl 1):49–61.
32. Matter MS, et al. Targeting the mTOR pathway in hepatocellular carcinoma: current state and future trends. J Hepatol. 2014;60(4):855–65.
33. Ferrin G, et al. Activation of mTOR signaling pathway in hepatocellular carcinoma. Int J Mol Sci. 2020;21(4):1266.

**Publisher's Note** Springer Nature remains neutral with regard to jurisdictional claims in published maps and institutional affiliations.